

# 1 PINGU: The Precision IceCube Next Generation 2 Upgrade

---

**Marek Kowalski\*** for the IceCube-PINGU collaboration

*Physikalisches Institut, Universität Bonn*

*E-mail:* [kowalski@physik.uni-bonn.de](mailto:kowalski@physik.uni-bonn.de)

The PINGU experiment, a planned low energy infill extension of the IceCube observatory, aims to provide a megaton-scale neutrino detector sensitive to  $O(10)$  GeV neutrinos. While the prime motivation stems from its ability to determine the neutrino mass hierarchy, such a detector would also have an unprecedented sensitivity to neutrinos from galactic Supernovae and low-mass WIMP annihilation. The performance of PINGU is discussed in terms of effective volume, energy and directional resolution, as well as the sensitivity for the determination of the neutrino mass hierarchy. Finally, we summarize the project status.

*XV Workshop on Neutrino Telescopes,  
11-15 March 2013  
Venice, Italy*

---

\*Speaker.

## 3 1. Introduction

4 Open ice/water Cherenkov neutrino detectors utilize transparent Antarctic ice or ocean/lake  
5 water to cost-effectively obtain large amounts of target material [1, 2, 3, 4]. The concept has  
6 already been successfully applied in the exploration of the high energy neutrino sky, with IceCube  
7 providing the first evidence of a high energy astrophysical neutrino flux [3, 5]. By increasing the  
8 density of instrumentation in the ice, the energy threshold of the neutrino detector can be lowered  
9 while still providing unprecedented large volumes. A successful example is DeepCore, which was  
10 installed as an infill array at the center of IceCube in the exceptionally clear ice between 2100 and  
11 2450 m below the surface. By lowering the energy threshold to  $\sim 20$  GeV the detector became  
12 sensitivity to neutrino oscillations, constraining  $\Delta m_{23}^2$  and  $\theta_{23}$  [6].

13 The sensitivity of megaton-sized atmospheric neutrino detectors to the neutrino mass hierar-  
14 chy (NMH) was pointed out in [7]. The requirement for the measurement is an energy threshold  
15 below 10 GeV, as well as an effective target mass of several megatons to obtain sufficient statistics  
16 of atmospheric neutrinos. The proposed PINGU detector is designed to enable the NMH measure-  
17 ment, as well as improve the sensitivity to neutrino mixing parameters, low energy WIMPs and  
18 galactic Supernovae. In this contribution, we focus on the NMH measurement.

19 The sensor technology and deployment strategy of PINGU builds on the experience gained  
20 with IceCube. One detector configuration that has been simulated in detail consists of 40 strings  
21 (instrumented cables), each carrying 60 light sensors (PINGU Digital Optical Modules), arranged  
22 as an even denser infill at the center of DeepCore (see Fig. 1). In the following, we discuss the  
23 performance of this particular detector and its sensitivity to the NMH. The project status is sum-  
24 marized in the last section.

## 25 2. Event Reconstruction and Effective Volumes

26 Because of the low energies involved, events relevant for PINGU are mostly contained inside  
27 the geometrical bounds of the detector. Depending on the neutrino flavor, they will have a some-  
28 what different topology: while  $\nu_e$  and the majority of  $\nu_\tau$  will appear as isolated particle showers  
29 (called cascades), generating light in a fuzzy Cherenkov cone, charged current (CC)  $\nu_\mu$  events will  
30 have an additional muon track. Since the emerging muon travels faster than the speed of light in ice,  
31 photons produced by the track can arrive earlier than the light from the initial vertex, and hence can  
32 be used to discriminate the two event topology. At low energies ( $E \lesssim 5$  GeV), separation becomes  
33 generally difficult due to the short muon track. Simulated events are reconstructed using a log-  
34 likelihood method adapted from IceCube that incorporates the different event types (cascade-like,  
35 track-like), as well as light propagation effects in the ice. Energy and angular resolution for CC  $\nu_\mu$   
36 events are shown in Fig. 2. Similar energy and angular resolution are found for CC  $\nu_e$  events, while  
37 somewhat worse resolution are obtained for  $\nu_\tau$ , as well as NC events due to the generally smaller  
38 visible energy.

39 To be included in the final analysis sample, simulated events are required to satisfy veto,  
40 containment (75 m radial distance from the detector central axis) and directional criteria ( $\theta_{\text{rec}} > 90^\circ$ ,  
41 all events are upward going). The resulting effective volume after all cuts is shown in Fig. 3.

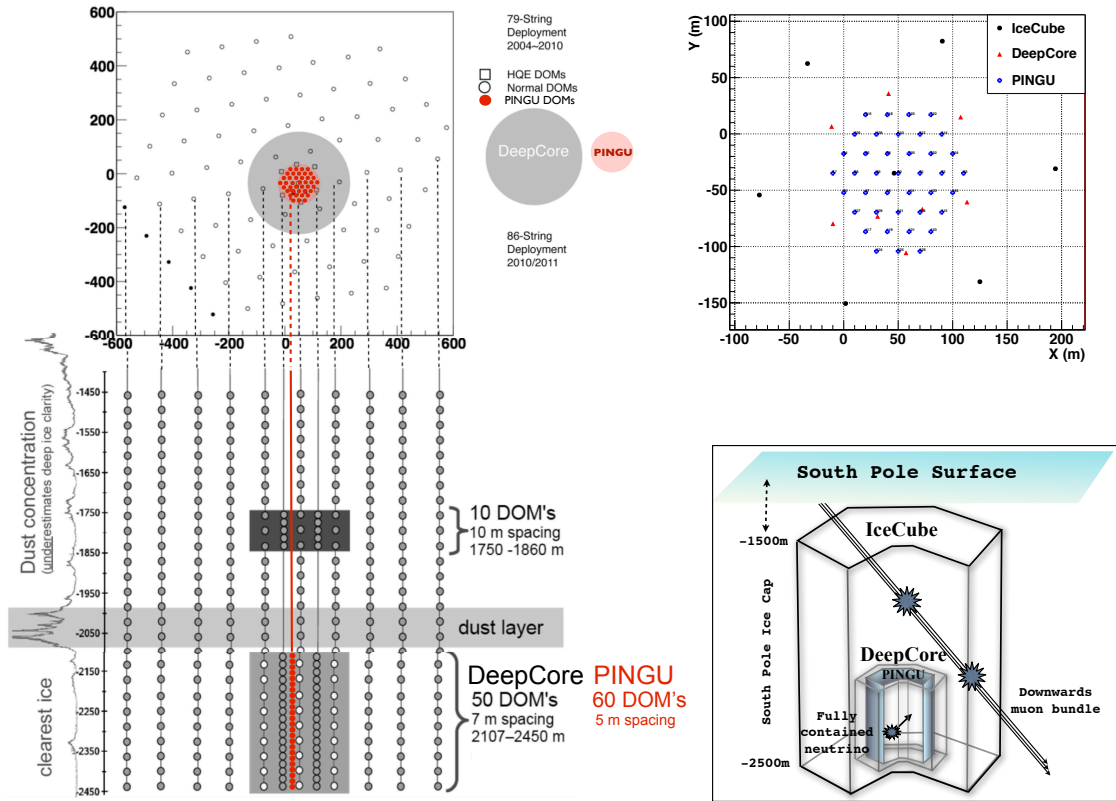


**Figure 1:** The left figure shows overhead and side views of the baseline 40-string PINGU detector. It also shows the surrounding IceCube and DeepCore strings, and vertical spacings for DeepCore and PINGU modules. In the interest of clarity, the side view only shows some of the strings. The leftmost curve along the side of the figure delineates the dust concentration in the ice, showing that PINGU will be located in the clearest ice. The top right figure shows an enlarged top view of the baseline 40-string geometry. The bottom right figure provides a sketch of a contained  $\nu_\mu$  CC event (signal) and a throughgoing muon bundle from a cosmic-ray air shower (one type of background, rarely coincident with neutrinos).

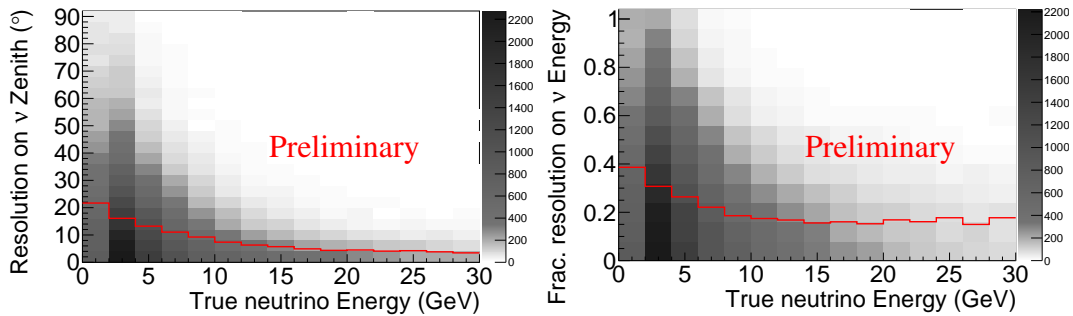


**Figure 2:** Zenith angle and fractional energy resolutions for  $\nu_\mu$  events with reconstructed vertices within the PINGU fiducial volume. The red line indicates the median value in each energy bin. The grey scale indicates number of simulated events in each bin.

POS (Neutel 2013) 056

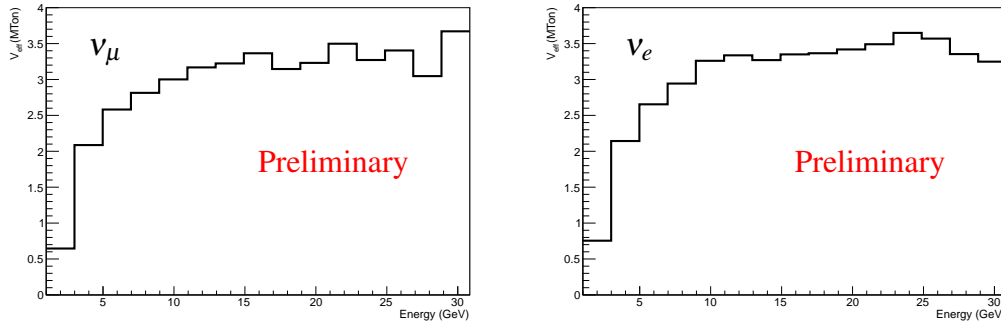


**Figure 3:** Effective volume for  $\nu_\mu$  (left) and  $\nu_e$  (right) events after final selection cuts.

### 42 3. Neutrino Mass Hierarchy

#### 43 3.1 Signature

44 The mixing angles and mass-squared differences that describe oscillations in the neutrino sec-  
 45 tor have been measured with high precision through the efforts of a variety of experiments world-  
 46 wide [8], while the mass ordering is still unknown. PINGU will be capable of determining this  
 47 mass ordering by virtue of its ability to collect a high-statistics sample of atmospheric neutrinos  
 48 in the energy range above a few GeV. The ordering, or mass hierarchy, is denoted “normal” (NH)  
 49 when  $\nu_3$  is the most massive of the three neutrino mass eigenstates and “inverted” (IH) if it is the  
 50 least. This ordering can be described in terms of the sign of mass-squared difference measured by  
 51 atmospheric neutrino oscillation experiments,  $\Delta m_{\text{atm}}^2$ , where  $\Delta m_{\text{atm}}^2 > 0$  corresponds to the normal  
 52 hierarchy and  $\Delta m_{\text{atm}}^2 < 0$  to the inverted.

53 Besides vacuum oscillations, there are two distinct physical effects that play a role as neutrinos  
 54 propagate through the Earth. The first is the MSW effect [9, 10] that results in an enhancement of  
 55 the oscillation probability for  $\nu_\mu \rightarrow \nu_e$  (NH), or  $\bar{\nu}_\mu \rightarrow \bar{\nu}_e$  (IH), and is strongly dependent on the  
 56 density along the flight path. The second effect arises from the density transition at the Earth’s  
 57 mantle-core interface, where neutrinos can undergo “parametric enhancement” of their oscillation  
 58 probability [11]. The aggregate effect of these phenomena on muon neutrinos, in both NH and IH  
 59 scenarios, is shown in Fig. 4. The survival probabilities of antineutrinos in the NH are essentially  
 60 identical to those of neutrinos in the IH, and vice versa. However, asymmetries in the cross sections  
 61 and kinematics of  $\nu$  and  $\bar{\nu}$  interactions with nuclei, along with the higher atmospheric flux of  
 62 neutrinos relative to antineutrinos, lead to different detected event rates depending on the hierarchy.  
 63 Therefore a precision measurement of the survival probabilities in the energy range targeted by  
 64 PINGU permits a determination of the NMH without explicit  $\nu - \bar{\nu}$  discrimination [12].

65 The impact of MSW effect and parametric enhancement on atmospheric neutrinos, and thus  
 66 the signal for determining the hierarchy, is illustrated in Fig. 5. The figure shows the difference  
 67 between the number of detected neutrino events per year under each hierarchy, after applying the  
 68 selection criteria and event reconstruction described above, scaled by the Poisson error on the  
 69 number of NH events to obtain something analogous to a  $\chi^2$  term. The plots are binned as a  
 70 function of the reconstructed neutrino energy,  $E_\nu$ , and the cosine of the reconstructed zenith an-  
 71 gle of the neutrino ( $\cos \theta_\nu$ ). To illustrate the individual contributions to the NMH signal,  $\nu_\mu$  and

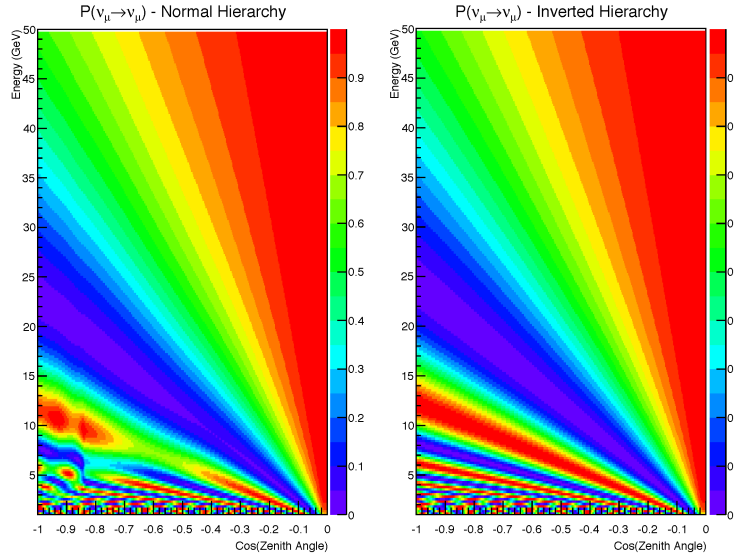


**Figure 4:** Muon neutrino survival probability after traveling through the earth, binned in both neutrino energy and cosine of the zenith angle. (A path directly through the center of the Earth corresponds to  $\cos \theta = -1$ .)

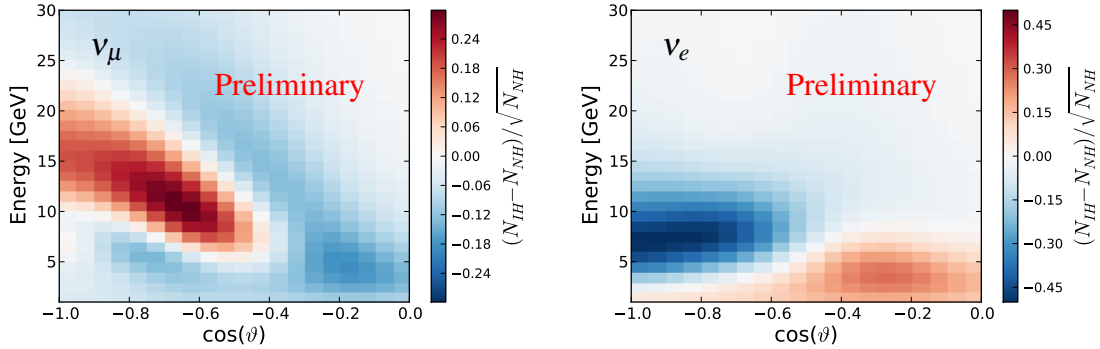


**Figure 5:** Distinguishability metric as defined in [7] for one year of simulated PINGU data. The sum of the absolute values of each bin in each plot gives an estimate of the number of  $\sigma$  separating the two hierarchies. The left figure shows track-like events from CC  $\nu_\mu$  interactions. The right figure shows  $\nu_e$  CC events. For illustrative purposes we assume perfect particle ID in creating these figures.

72  $\nu_e$  are shown separately, i.e., assuming perfect flavor identification ( $\nu_\tau$  is contributing less to the  
 73 signal). One finds regions in which the number of events expected for the NH is greater than that  
 74 expected for the IH (blue regions) and vice-versa (red regions). Sensitivity to this pattern of the  
 75 event number differences as a function of  $E_\nu$  and  $\cos \theta_\nu$  permits determination of the neutrino mass  
 76 hierarchy. This “distinguishability” metric [7] is relevant for understanding the regions of interest  
 77 in the energy-angle space from which useful information may be extracted, and can be used to cal-  
 78 culate a rough approximation of the PINGU sensitivity to the NMH. More detailed simulations and  
 79 analysis methods are then used to determine the sensitivity with improved accuracy, as discussed  
 80 below.

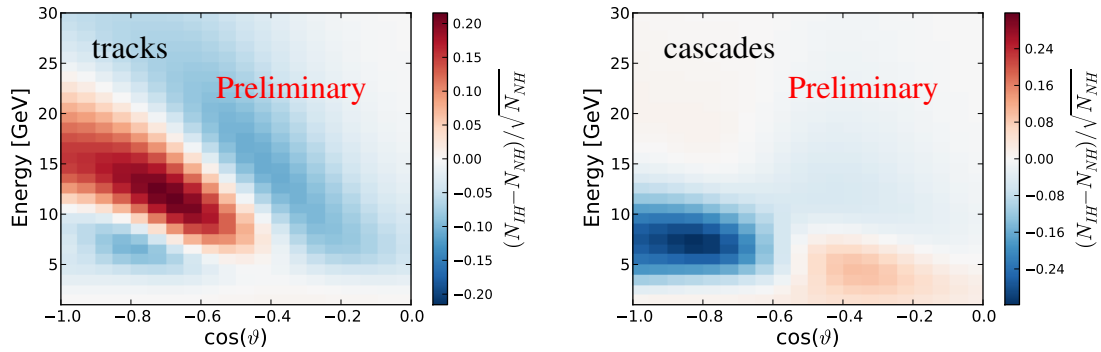


**Figure 6:** Distinguishability metric as defined in [7] for one year of simulated PINGU data with reconstruction and particle identification applied. The left panel shows track-like events (mostly due to CC  $\nu_\mu$ ) while the right shows cascade-like events (mostly  $\nu_e$  and  $\nu_\tau$  CC events, as well as NC events from any neutrino flavors).

### 81 3.2 Analysis

82 The analysis is performed on atmospheric neutrinos with fluxes as predicted by [13], which  
 83 are tracked through the Earth using a full three-flavor formalism including matter effects based on  
 84 the standard PREM model of the Earth [14]. The simulated neutrino events are all reconstructed  
 85 without regard to neutrino flavor and employ a basic algorithm for particle identification (PID) to  
 86 separate track-like events produced by  $\nu_\mu$  CC interactions from cascade-like events produced by  $\nu_e$   
 87 CC,  $\nu_\tau$  CC, and all-flavor NC interactions. In Fig. 6 we show the distinguishability metric evaluated  
 88 for the track and cascade channel, where the energy-dependent PID efficiency is parametrized using  
 89 a full simulation and reconstruction of simulated data.

90 Three independent analyses were employed in studying PINGU’s sensitivity to the NMH. The  
 91 most detailed method uses a library of simulated events to generate the distribution of  $E_\nu$  and  $\cos\theta_\nu$   
 92 expected from different possible combinations of true oscillation parameters, generates ensembles  
 93 of pseudo-experiments for these scenarios and uses a likelihood ratio method to determine the de-  
 94 gree to which one hierarchy is favored. The second analysis likewise starts with the same library  
 95 of simulated events, but uses the so-called “Asimov” approximation instead of generating ensem-  
 96 bles of pseudo-experiments for every possible combination of oscillation parameters [15]. This  
 97 technique essentially assumes that statistical fluctuations in the experimental data are as likely to  
 98 reinforce as to obscure the signature of the correct hierarchy, such that only the single most prob-  
 99 able set of data for any given set of parameters needs to be analyzed. A  $\chi^2$  statistic can then be  
 100 calculated between the assumed true distribution and every alternate set of observables. Systematic  
 101 uncertainties are incorporated as nuisance parameters to be fit simultaneously, and the significance  
 102 of the hierarchy is determined from the  $\Delta\chi^2$  between the best fits in the subspaces corresponding  
 103 to normal and inverted hierarchies.

104 The third analysis, from which the results presented here were derived, uses the simulated  
 105 events to build a parametrized model of the detector response. This includes effective volumes,  
 106 analysis selection efficiency, reconstruction resolutions and biases, and the particle identification  
 107 efficiency, similar to the procedure used in [16, 12, 7]. At the heart of the method lies the Fisher

108 information matrix, consisting of the partial derivatives of the event counts in each bin with respect  
 109 to all parameters under study (calculated numerically) for the true parameters, weighted by the  
 110 statistical errors:

$$F_{kl} = \sum_i \frac{1}{\sigma_{n_i}^2} \frac{\partial n_i}{\partial p_k} \frac{\partial n_i}{\partial p_l}. \quad (3.1)$$

111 Here  $p_k, p_l$  denote the parameters with index  $k$  and  $l$ , while  $n_i$  is the expected number of events  
 112 in bin  $i$  and  $\sigma_{n_i} = \sqrt{n_i}$  the corresponding uncertainty. Inverting the Fisher matrix yields the full  
 113 covariance matrix between the parameters of interest, while the statistical uncertainty of param-  
 114 eter  $i$  is given by  $1/\sqrt{F_{ii}}$ . Since all parameters must be continuous to be incorporated, the mass  
 115 hierarchy is represented by a parameter  $h$ , linearly incorporating the observed event counts in each  
 116 bin according to  $n_i^{obs} = hn_i^{true} + (1-h)n_i^{alt}$ . The significance of the NMH measurement is given by  
 117  $1/\sigma_h$ , where  $\sigma_h$  follows from the inverted Fisher matrix.

118 The advantages of this method are the simplicity and small computational demands with which  
 119 one can include a large number of systematic errors through nuisance parameters. Another advan-  
 120 tage arises from the fact that the analysis is not limited by the size of the available Monte Carlo  
 121 event library. Although the event library corresponds to approximately 5 years of actual data, there  
 122 is evidence that statistical noise in the expected distributions causes a systematic upward bias [17]  
 123 in the significances predicted by the first two analyses described above, that is not present in the  
 124 parametric Fisher information matrix method.

125 The derivatives for the other parameters are obtained numerically and, in the range of interest,  
 126 the linear approximation of the parameter dependence is sufficiently accurate (as previously shown  
 127 in [18]). Only the CP-violating phase,  $\delta_{CP}$ , can not be incorporated reliably in this approach, due  
 128 to the lack of external constraints on its value, but PINGU is expected to have low sensitivity to  
 129 this parameter [7], which we have verified using the LLR analysis. Since the dependence of the  
 130 hierarchy measurement on  $\delta_{CP}$  is small, we fix  $\delta_{CP} = 0$ . Strong covariance of another parameter  
 131 with the hierarchy parameter would indicate that there is a potentially important systematic which  
 132 might affect our ability to measure the hierarchy.

133 When examining the same sets of external nuisance parameters and after accounting for the  
 134 bias due to limited Monte Carlo statistics, we have found that the results from the Fisher infor-  
 135 mation matrix agrees well with the Asimov Monte Carlo simulation approach. We are therefore  
 136 confident that the parametric approximations used in this analysis are reliable, and use it to incor-  
 137 porate a wider variety of systematics and determine the sensitivity of PINGU to the hierarchy for  
 138 longer exposures than can be estimated using Monte Carlo-based methods.

### 139 3.3 Systematics and Results

140 The neutrino oscillation pattern appearing in the PINGU detector arises from the wide range  
 141 of atmospheric neutrino energies and baselines to which PINGU is sensitive. PINGU has suffi-  
 142 cient energy and angular resolutions to determine the NMH, and it is shown in the following that  
 143 detector-related systematics are not expected to impact the oscillation pattern in such a way as to  
 144 induce a hierarchy misidentification. We categorize as a second broad class of systematics those  
 145 arising from uncertainties in externally measured values of neutrino fluxes and oscillation param-  
 146 eters. In the following we describe and quantify each of these systematics, and indicate possible  
 147 ways to better constrain them to reduce their impact on the final significance.



148 The external systematics studied include uncertainties in the atmospheric neutrino flux and  
 149 spectral index,  $\Delta m_{12}^2$ ,  $\sin^2(\theta_{12})$ ,  $\Delta m_{23}^2$ , and  $\sin^2(\theta_{23})$ . Relevant detector-related systematics studied  
 150 so far include uncertainties in the absolute energy scale (*i.e.*, energy calibration), a scale factor and  
 151 energy-dependent shift in the effective volume, as well as uncertainties in the neutrino interaction  
 152 cross sections (both for neutrinos and anti-neutrinos). Some detector uncertainty parameters are  
 153 degenerate with each other, such as the scale factors applied to the atmospheric neutrino flux,  
 154 effective volume and cross-sections, and therefore we only include one of these uncertainties. On  
 155 the other hand, the flux and cross-section are different for neutrinos and anti-neutrinos. Since  
 156 the signal depends on the difference between neutrinos and anti-neutrino events, one needs to  
 157 treat these two systematics separately. Although MINERvA [19] results will likely reduce the  
 158 uncertainties on the relevant cross-sections substantially by the time of the PINGU data analysis,  
 159 we have added a conservative Gaussian uncertainty of 15% on possible scale factors for neutrino  
 160 and anti-neutrino cross-sections. The cross-section, the effective volume, or the flux can show an  
 161 energy dependence that is not properly modeled; we include this possibility by adding an extra  
 162 linear energy dependence of the effective volume, such that  $V_{\text{eff}}^{\text{sys}}(E_\nu) = V_{\text{eff}}(E_\nu)(1 + \varepsilon E_\nu)$ , where  
 163  $\varepsilon$  is a nuisance parameter determined by the data. The list of systematic uncertainties investigated  
 164 so far is extensive but not complete. For instance, the impact of uncertainties in the optical ice  
 165 properties still needs to be studied although calibration devices to be deployed as part of PINGU  
 166 will reduce them considerably compared to their present values.

167 The effect of the systematic uncertainties on the event rates is parametrized, providing one  
 168 linear (nuisance) parameter for each source. The Fisher information matrix is then evaluated in-  
 169 cluding the systematic uncertainties, leading to a significance of  $1.75\sigma$  with the first year of data.  
 170 Figure 7 illustrates the “impact” of the individual sources of uncertainty, defined as the increase in  
 171 significance seen when a particular uncertainty is disabled in the analysis. The figure also indicates  
 172 that the combined effect of individual detector-specific uncertainties studied so far is moderate and  
 173 generally dominated by the combined physics-related uncertainties. Our studies indicate that the  
 174 measurement is limited by systematics and that the significance will grow slightly more slowly than  
 175  $\sqrt{t}$  on the time scale of a few years. The resulting significance as a function of the amount of data  
 176 taken by the full detector is summarized in Fig. 8, assuming  $\theta_{23}$  is in the first octant. If instead  $\theta_{23}$   
 177 is in the second octant, the significance with which one can determine the NMH would be nearly a  
 178 factor two larger.

179 There are a number of future improvements that we believe will further increase the signifi-  
 180 cance. Two promising ones are better particle ID and the use of the reconstructed inelasticity of  
 181 the neutrino event, which is a weak  $\nu/\bar{\nu}$  discriminator. More sophisticated particle ID will enable  
 182 better exploitation of the distinct patterns of  $\nu_\mu$  events relative to those of  $\nu_e$  and  $\nu_\tau$ . The use of the  
 183 inelasticity would help us distinguish neutrinos from antineutrinos on a statistical basis and could  
 184 provide a 20-50% increase in significance [20, 21]. Other lines of investigation include geometry  
 185 optimization, improved event selection efficiency and more accurate event reconstruction.

#### 186 4. Project Status and Outlook

187 The IceCube-PINGU collaboration consists of the IceCube collaborators, with several new  
 188 and associated groups focusing on the low-energy infill extension. A Letter of Intent has been



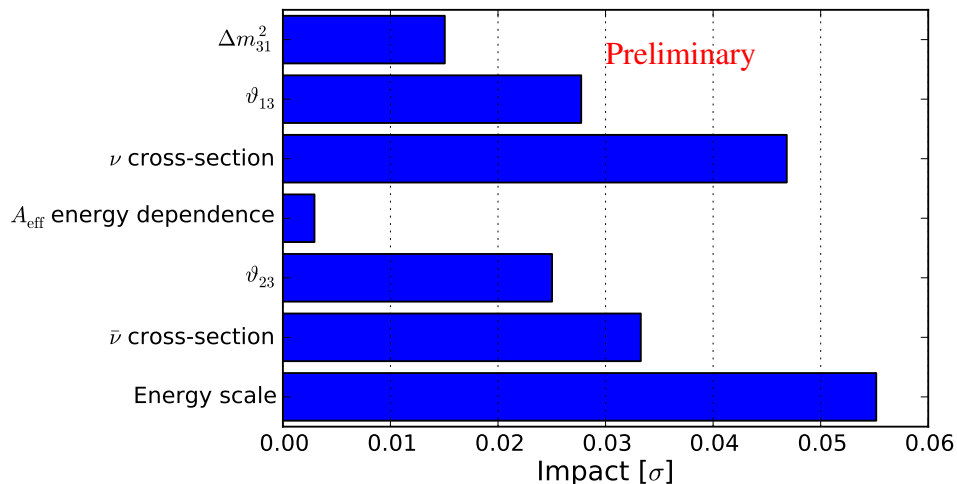


**Figure 7:** Summary of the systematic errors, their assumed variations, and their impacts on the estimated one-year significance of the mass hierarchy measurement. See text for details.

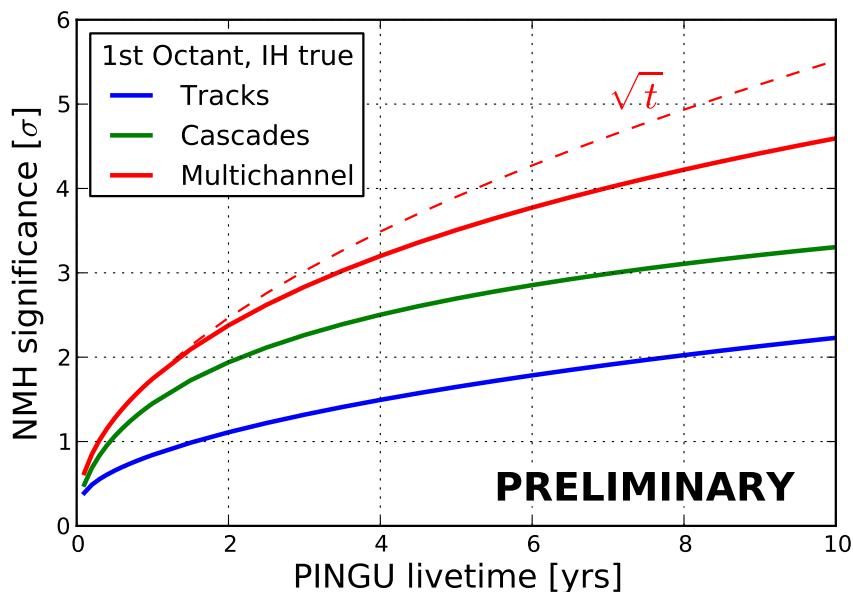


**Figure 8:** Significance of the neutrino mass hierarchy determination as a function of time, using the Fisher/Asimov approach and a full complement of systematics (see text for details). Note the red dashed line shows the expectation for a  $\sqrt{t}$  dependence.

189 submitted in December 2013, containing a NMH sensitivity study for the 40-string geometry, as  
 190 well as covering a range of other science opportunities for PINGU. Photodetectors, communication  
 191 and ice drilling technology are based on existing IceCube technology, with a high degree of present

192 readiness. Assuming that funding can be secured in 2014, installment of the detector at the South  
193 Pole could start in 2018 and be completed by 2020.

## 194 References

- 195 [1] J. Zornoza *et al.*, “Antares results”, contribution to this conference, 2013.
- 196 [2] P. SAPIENZA *et al.*, “Km3Net perspective”, contribution to this conference, 2013.
- 197 [3] A. Karle *et al.*, “Icecube”, contribution to this conference, 2013.
- 198 [4] U. Katz *et al.*, “Orca”, contribution to this conference, 2013.
- 199 [5] M. Aartsen *et al.*, “Evidence for High-Energy Extraterrestrial Neutrinos at the IceCube Detector”,  
200 *Science* **342** (2013) 1242856, [arXiv:1311.5238](https://arxiv.org/abs/1311.5238).
- 201 [6] M. Aartsen *et al.*, “Measurement of Atmospheric Neutrino Oscillations with IceCube”,  
202 *Phys.Rev.Lett.* **111** (2013) 081801, [arXiv:1305.3909](https://arxiv.org/abs/1305.3909).
- 203 [7] E. K. Akhmedov, S. Razzaque, and A. Y. Smirnov, “Mass hierarchy, 2-3 mixing and CP-phase with  
204 Huge Atmospheric Neutrino Detectors”, *JHEP* **1302** (2013) 082, [arXiv:1205.7071](https://arxiv.org/abs/1205.7071).
- 205 [8] J. Beringer *et al.* (Particle Data Group), *Phys. Rev. D* **86** (Jul, 2012) 010001.
- 206 [9] L. Wolfenstein, *Phys.Rev.* **D17** (1978) 2369–2374.
- 207 [10] S. Mikheyev and A. Y. Smirnov, *Prog.Part.Nucl.Phys.* **23** (1989) 41–136.
- 208 [11] E. K. Akhmedov, A. Dighe, P. Lipari, and A. Y. Smirnov, “Atmospheric neutrinos at  
209 Super-Kamiokande and parametric resonance in neutrino oscillations”, *Nucl.Phys.* **B542** (1999) 3–30,  
210 [hep-ph/9808270](https://arxiv.org/abs/hep-ph/9808270).
- 211 [12] O. Mena, I. Mocioiu, and S. Razzaque, “Neutrino mass hierarchy extraction using atmospheric  
212 neutrinos in ice”, *Phys. Rev. D* **78** (2008) 093003.
- 213 [13] M. Honda, T. Kajita, K. Kasahara, S. Midorikawa, and T. Sanuki, “Calculation of atmospheric  
214 neutrino flux using the interaction model calibrated with atmospheric muon data”, *Phys.Rev.* **D75**  
215 (2007) 043006, [astro-ph/0611418](https://arxiv.org/abs/astro-ph/0611418).
- 216 [14] A. Dziewonski and D. Anderson, “Preliminary reference earth model”, *Phys.Earth Planet.Interiors* **25**  
217 (1981) 297–356.
- 218 [15] G. Cowan, K. Cranmer, E. Gross, and O. Vitells, “Asymptotic formulae for likelihood-based tests of  
219 new physics”, *Euro. Phys. J. C* **71** (2010) 1554.
- 220 [16] W. Winter, “Neutrino mass hierarchy determination with IceCube-PINGU”, *Phys.Rev.* **D88** (2013)  
221 013013, [arXiv:1305.5539](https://arxiv.org/abs/1305.5539).
- 222 [17] R. J. Barlow and C. Beeston, “Fitting using finite Monte Carlo samples”, *Comput.Phys.Commun.* **77**  
223 (1993) 219–228.
- 224 [18] E. Ciuffoli, J. Evslin, and X. Zhang, “Confidence in a Neutrino Mass Hierarchy Determination”,  
225 [arXiv:1305.5150](https://arxiv.org/abs/1305.5150).
- 226 [19] L. Aliaga *et al.*, “Design, Calibration, and Performance of the MINERvA Detector”,  
227 [arXiv:1305.5199](https://arxiv.org/abs/1305.5199).
- 228 [20] M. Ribordy and A. Y. Smirnov, “Improving the neutrino mass hierarchy identification with inelasticity  
229 measurement in PINGU and ORCA”, *Phys.Rev.* **D87** (2013) 113007, [arXiv:1303.0758](https://arxiv.org/abs/1303.0758).
- 230 [21] A. Smirnov, “Mass hierarchy and matter effects”, contribution to this conference, 2013.